NASA/TM-2002-21071

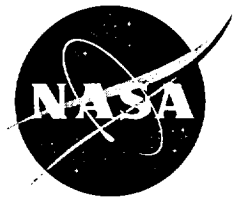

Ground and Flight Evaulation of a Small-Scale Inflatable-Winged Aircraft

James E. Murray , Joseph W. Pahle, Stephen V. Thornton, Shannon Vogus
NASA Dryden Flight Research Center
Edwards, California

Tony Frackowiak
Analytical Services & Materials, Inc.
Hampton, Virginia

Joe Mello
California Polytechnic University
San Luis Obispo, California

Brook Norton
Vertigo, Inc.
Lake Elsinore, California

National Aeronautics and
Space Administration

Dryden Flight Research Center
Edwards, California 93523-0273

January 2002

NOTICE

Use of trade names or names of manufacturers in this document does not constitute an official endorsement of such products or manufacturers, either expressed or implied, by the National Aeronautics and Space Administration.

Available from the following:

NASA Center for AeroSpace Information (CASI)
7121 Standard Drive
Hanover, MD 21076-1320
(301) 621-0390

National Technical Information Service (NTIS)
5285 Port Royal Road
Springfield, VA 22161-2171
(703) 487-4650

GROUND AND FLIGHT EVALUATION OF A SMALL-SCALE INFLATABLE-WINGED AIRCRAFT

James E. Murray*, Joseph W. Pahle*, Stephen V. Thornton†, Shannon Vogus‡
NASA Dryden Flight Research Center
Edwards, California

Tony Frackowiak§
Analytical Services & Materials, Inc.
Hampton, Virginia

Joseph D. Mello, PhD¶
California Polytechnic University
San Luis Obispo, California

Brook Norton**
Vertigo, Inc.
Lake Elsinore, California

Abstract

A small-scale, instrumented research aircraft was flown to investigate the flight characteristics of inflatable wings. Ground tests measured the static structural characteristics of the wing at different inflation pressures, and these results compared favorably with analytical predictions. A research-quality instrumentation system was assembled, largely from commercial off-the-shelf components, and installed in the aircraft. Initial flight operations were conducted with a conventional rigid wing having the same dimensions as the inflatable wing. Subsequent flights were conducted with the inflatable wing. Research maneuvers were executed to identify the trim, aerodynamic performance, and longitudinal stability and control characteristics of the vehicle in its different wing configurations. For the angle-of-attack range spanned in this flight program, measured flight data demonstrated that the rigid wing was an effective simulator of the lift-generating capability of the inflatable wing. In-flight inflation of the wing was demonstrated in three flight operations, and measured flight data illustrated the dynamic characteristics during wing inflation and transition to controlled lifting flight. Wing inflation was rapid and the vehicle dynamics during inflation and transition were benign. The resulting angles of attack and of sideslip were small, and the dynamic response was limited to roll and heave motions.

Nomenclature

α	angle of attack, deg
β	angle of sideslip, deg
a_n	normal acceleration, g
CG	center of gravity
C_{m_α}	longitudinal stability parameter, 1/deg
$C_{m_{\delta e}}$	symmetric elevon control effectiveness parameter, 1/deg
C_N	normal force coefficient
C_{N_α}	normal-force curve slope parameter, 1/deg
COTS	commercial off-the-shelf
EMI	electromagnetic interference
GPS	Global Positioning System
g	acceleration of gravity
mg	vehicle weight, lb
NASA	National Aeronautics and Space Administration

* Aerospace Engineer, member.

† Branch Chief.

‡ Aerospace Engineer.

§ Aerospace Technician.

¶ Associate Professor.

**Technologies Program Manager, member.

POPU	pushover-pullup
psig	pounds per square inch gage
$\bar{q}$	dynamic pressure, lb/ft^2
R/C	radio control
S_{ref}	reference area, ft^2

Introduction

Inflatable structures have been considered for and applied to a number of aerospace applications. Early designers[1] considered pressurized tubular structures to carry some of the aerodynamic flight loads. In the 1950s, inflatable aircraft designs, including the Goodyear Inflatoplane[2-4] and the ML Aviation Utility[5] were fabricated using pressurized airfoil shapes in which a noncylindrical shape was maintained by internal tension members. These low-pressure systems included external bracing to carry some of the aerodynamic loads. In the 1960s, a reentry vehicle concept[6] was proposed using inflatable tubular structures. Recent concepts include both baffled, segmented wing designs[7] and designs using multiple pressurized spars to roughly define the airfoil shape and to carry the aerodynamic loads.[8] Material and fabrication advances have allowed current designs[9, 10] to operate at high inflation pressure and support fully cantilevered aerodynamic loads, and several applications have been demonstrated in flight.[11]

Inflatable wings produced for previously completed U.S. Navy research and development were made available to researchers at NASA Dryden Flight Research Center. These inflatable wings were integrated into the design of two small-scale (15-25 lb), instrumented, research aircraft configurations: a pusher-powered conventional configuration (I-2000), and an unpowered winged lifting-body configuration. Only the results from the I-2000 are contained in this paper. Conventional ground and flight test techniques were applied to this research aircraft to gain an understanding of the structural, aerodynamic, and operational characteristics of vehicles with state-of-the-art inflatable wings.

Ground and flight testing of inflatable structures at small scale is attractive for several reasons. Most ground and flight test operations are greatly simplified when the mass of the test vehicle is low. Vehicle fabrication costs, personnel costs, and test range costs are all reduced with smaller vehicles. Furthermore, the maturation of miniaturized sensor technology, Global Positioning System (GPS) receivers, and micro-controller hardware by the electronics industry has enabled research-quality instrumentation systems onboard small-scale vehicles with only a modest weight, power, and cost impact.

This paper presents the results of ground and flight tests applied to a small-scale, research aircraft with an inflatable wing. The inflatable wing and aircraft configuration are briefly described. Data from static load tests are compared with analytical results for the wing alone. Development of an inflation system, wing stowage and retention system, and research instrumentation are described. Data from the onboard research instrumentation system are used to compare the trim, performance, and stability and control characteristics of the vehicle when configured with the inflatable wing and with a similar rigid wing. Finally, flight data and ground-based photo images are used to illustrate the dynamic characteristics of the vehicle during in-flight wing inflation and transition to controlled lifting flight. Notice: Use of trade names or names of manufacturers in this document does not constitute an official endorsement of such products or manufacturers, either expressed or implied, by the National Aeronautics and Space Administration.

Inflatable Wing Description

The inflatable wings used in this program were designed and fabricated by Vertigo, Inc. (Lake Elsinore, California) for a U.S. Navy program. The inflatable wings fabricated for this U.S. Navy program were provided to NASA Dryden at no cost, and two research vehicles were designed around these wings. Figure 1 shows a simplified schematic of the wing.

The inflatable wing contains five inflatable, cylindrical spars that run spanwise from tip to tip. The spars are made of spirally braided Vectran threads (a Celanese AG product) laid over a urethane gas barrier. A fabric webbing spar cap is aligned on the top and bottom of each of the spars. The wing span is 64 in. tip to tip, and the chord is 7.25 in. The airfoil is a relatively thick, symmetric section NACA-0021. The wing does not contain any control surfaces. A manifold at the center of the wing holds the wing spars in position and provides a rigid connection between the high-pressure gas source (150 psig to 300 psig) and the

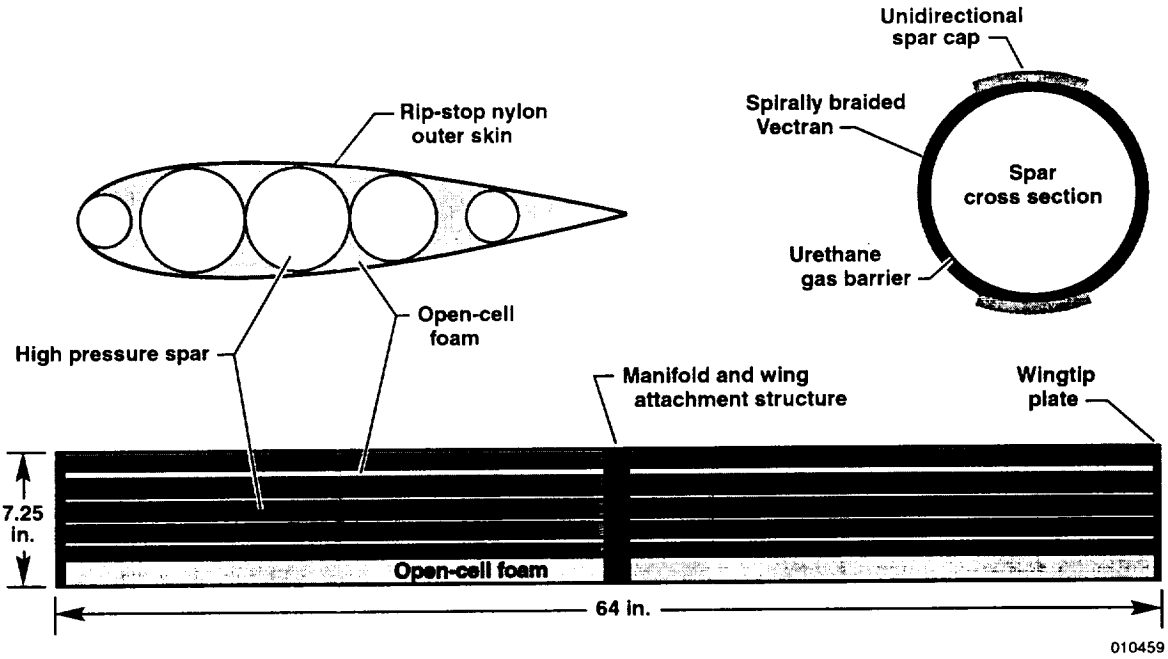

Figure 1. Inflatable wing structure.

wing spars. Once in the manifold, the high-pressure gas passes into each spar through an inflation pin that is mounted in the manifold. Between the spars and to the trailing edge of the wing is open-cell foam bonded to the spars and to a rip-stop nylon outer skin. Additionally, a rib at each tip rigidly connects all the spars to establish wing torsional stiffness. Thermally activated adhesives are used to bond the spars, foam, and the nylon skin into a contiguous wing structure.

I-2000 Vehicle Description

To evaluate a small-scale inflatable wing, a research aircraft designated the I-2000 was designed and built. The I-2000 research vehicle, shown in figure 2, is a fairly conventional aircraft configuration. This vehicle was designed to maximize operational flexibility and the quality of research data obtained in the flight program. The vehicle was designed for flight as either a powered configuration capable of conventional takeoff and landing, or as an unpowered glider configuration capable of being air-launched from a separate, powered carrier aircraft. The powered I-2000 was designed as a pusher to leave the nose clear for an airdata probe and maximize the quality of the airdata measurements. The fuselage was made large and boxlike to allow the freedom to install the onboard systems, including instrumentation, fuel tanks, uplink control hardware, and wing-inflation systems. The vehicle was configured with a large, rigid H-tail with large control surfaces (2 elevons and 2 rudders) to enhance stability, damping, and control authority, as well as to facilitate integration of the I-2000 with a carrier aircraft for air-launched operations. Because the inflatable wings had no control surfaces, full three-axis control was effected only by the tail control surfaces; the symmetric elevon controlled pitch, the differential elevon controlled roll, and the symmetric rudder controlled yaw.

The I-2000 was capable of flight in any one of three wing configurations: *rigid wing*, a conventional foam-and-fiberglass wing using geometry identical to that of the inflatable wing, *preinflated wing*, a wing inflated on the ground prior to flight, or *in-flight inflated wing*, a wing capable of inflation while in flight. Conversion among the three wing configurations was facilitated by fabricating multiple wing-deck assemblies to mate with the fuselage assembly The fuselage assembly contained the primary aircraft systems, while each wing-deck assembly held the remaining systems required to support the specific wing configuration (e.g. inflation system hardware). Longitudinal center-of-gravity (CG) locations were identical for all configurations, although the vertical CG location did vary with

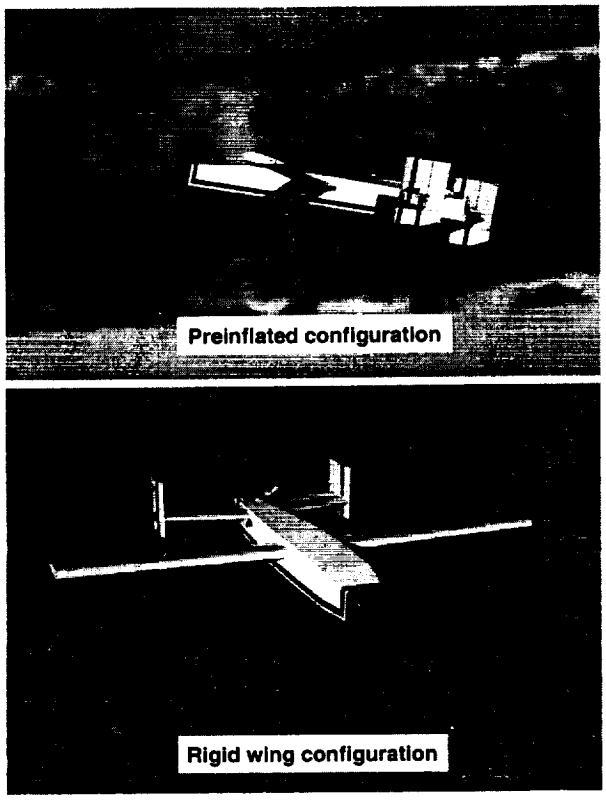

Figure 2. I-2000 research vehicle.

configuration. Vehicle weight ranged from 11.0 to 15.7 lb throughout the flight program.

Inflatable Wing Structural Testing

To structurally characterize the inflatable wing in preparation for flight testing, a series of static load tests was conducted. The wing was mounted at the centerline by clamping the inflation manifold in a rigid fixture (fig 3). Wing inflation pressure was supplied by regulated gaseous nitrogen. The loads were applied symmetrically and vertically at the wingtips using linear electromechanical actuators. Preliminary tests were conducted to determine the shear center of the wing. The actuators were then moved to the shear center position at the wingtips to induce a bending load with no torsional component. The applied loads were measured using load cells and recorded on a personal computer-based data acquisition system. Wingtip deflections were monitored with linear displacement sensors.

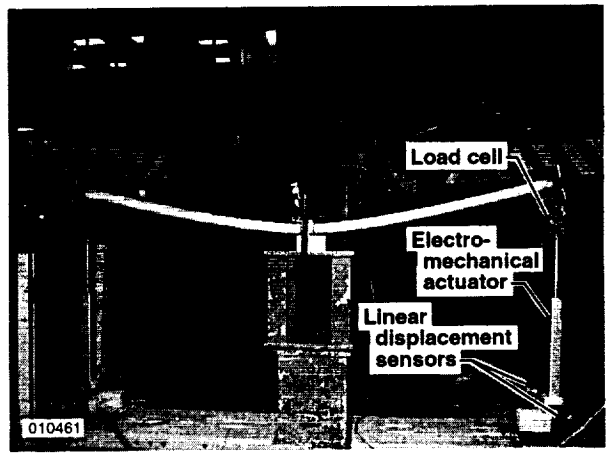

Figure 3. Static structural testing of the inflatable wing.

Loading tests were conducted using three different wing inflation pressures: 150 psig, 225 psig, and 300 psig. Figure 4 presents the test results for the left wing panel. Beginning at zero load and zero deflection, there is a characteristic and almost linear increase of load with increasing deflection for the first portion of the curve, followed by a significant reduction in slope out to the maximal load and deflection. The return path to the unloaded condition creates a hysteresis loop, with load being somewhat less for the decreasing load condition than for the increasing load condition at the same deflection. The physical mechanism that creates the hysteresis loop is unknown. Visual inspection during

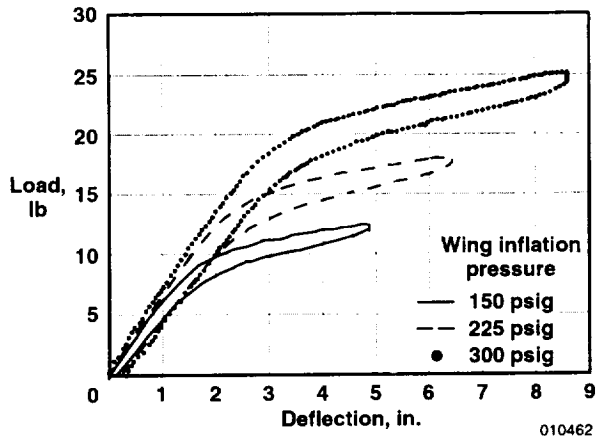

Figure 4. Left wingtip load as a function of wingtip deflection.

the testing confirmed that wrinkles in the spar tubes formed (or relaxed) at the wing root during the period of slope change.

Inflatable Wing Structural Analysis

A brief analytical study was conducted to complement the inflatable wing testing. The purpose of this work was to investigate analytical and computational structural models that might be applicable to this type of structure. The results offer some insight into wing behavior and some appropriate analysis and modeling techniques.

During the structural testing, inspection of the structure while under load and a study of test data led to the following observations. These are key in understanding the behavior and the subsequent development of appropriate modeling techniques.

- The initial (linear) stiffness of the wing is nearly the same throughout the range of inflation pressures tested.
- The load at which the onset of wrinkling occurs appears to be a linear function of inflation pressure.
- Inspection under the wing covering and foam in the root region, during tests, revealed that the spar caps in the upper tubes wrinkle progressively in the nonlinear range of the wingtip load as a function of displacement.

Two basic modeling approaches were investigated: a mechanics of materials analytical approach and a finite element approach. Only the results of the mechanics of materials analytical approach are presented. Many researchers[12-14] have successfully employed mechanics of materials methods to inflated structures similar to the inflatable wing; this work was limited to single tubes or structures in general. In the present work these methods were extended to the multi-spar configuration of the inflatable wing. Also, previous work employed homogeneous, isotropic, constant cross section structures. Because the composite micromechanics of the material and structure of the inflatable wing spar was more complicated, and because of the complex and progressive nature of the 5-tube response, the governing equations were coded in a MATLAB script file to analytically predict the behavior.

Figure 5 shows these results from the mechanics of materials analytical approach compared to test data. The model captures three salient characteristics of the test data: the pre-wrinkle or initial linear slope (which is independent of inflation pressure), the slope change at onset of wrinkling, and the linear increase in intial wrinkle load with inflation pressure. The model slightly underpredicts the stiffness of the structure in the linear region and overpredicts the post-wrinkle deflection. From these results, it appears that the inflated wing structure can be modeled effectively. A mechanics of materials type approach seems robust and is recommended for preliminary wing design. The methods developed here could possibly be extended to

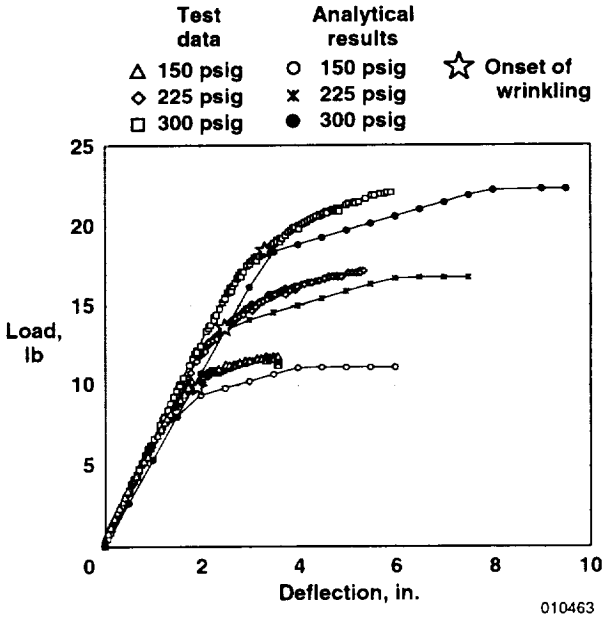

Figure 5. Analytical results compared to test data for wingtip load as a function of deflection.

include torsion and the superposition of bending and torsion. However, it may be more economical to investigate simplified finite-element models for these other loading types.

To accurately model the nonlinear response of such a structure beyond the onset of wrinkling would require additional testing and computational development. A specialized finite-element model and a material model may be required to deal with the inherent numerical stability problems for such a structure.

Inflation Gas Subsystem Design and Testing

Selection of wing inflation pressure was based on the results of the static structural characterization of the inflatable wing. The wingtip load corresponding to the onset of wrinkling was determined for each inflation pressure tested (fig 5). Assuming an elliptical wing lift distribution and a 15-lb vehicle gross weight, the vehicle load factor corresponding to the wingtip load at the onset of wrinkling was calculated. Figure 6 shows the vehicle load factor at onset of wrinkling as a function of inflation pressure. Based on these results, a minimum wing inflation pressure of 180 psig was selected for most flight operations to allow for a 3.5-*g* envelope.

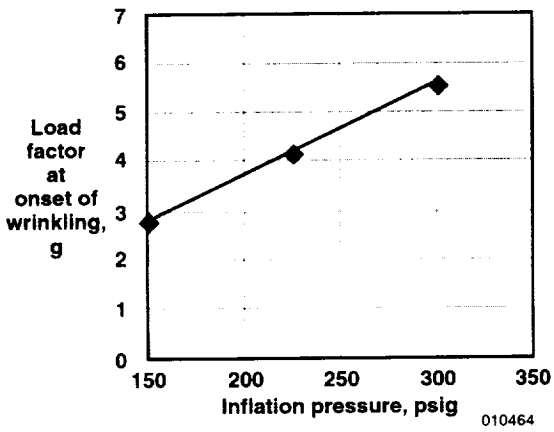

Figure 6. Allowable load factor as a function of wing inflation pressure.

Laboratory testing measured the wing leak-rate under the expected flight load, vibration, and temperature conditions. The results allowed appropriate sizing of the onboard inflation gas subsystem for the expected flight duration. A small commercial off-the-shelf (COTS) pressure vessel with a volume of approximately 35 in^3 was selected as the high-pressure source tank. This vessel was mated with a COTS adjustable regulator that included an integrated fill port, pressure relief plug, and manually-actuated source valve (fig 7). The output of the integrated regulator assembly was connected to the wing inflation manifold. Dry nitrogen was used for all ground and flight tests.

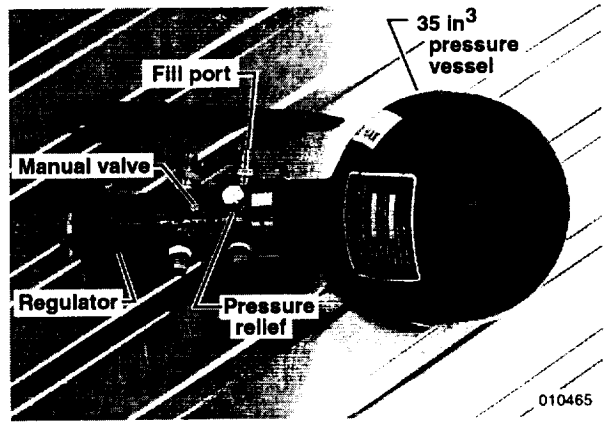

Figure 7. Inflation gas subsystem pressure vessel and regulator.

The same inflation gas subsystem was used for both pre-inflated flights and for in-flight inflation operations. When configured for pre-inflated flights, the wing was slowly inflated on the ground and only the final wing pressure was important. For these flights, the regulator pressure was set at the desired wing pressure (180 to 240 psig), and the high-pressure source tank was pressurized before flight to approximately 500 psig. The excess gas in the high-pressure source tank was then available during flight to make up any losses in the system resulting from leakage.

When configured for in-flight inflation, the inflation gas subsytem was required to control both the final wing pressure and the wing inflation rate. In this configuration, the adjustable regulator was effectively used as an adjustable orifice and the wing inflation system was a *blow down* (unregulated) system. Final wing pressure was controlled exclusively by the initial pressure in the high-pressure source tank; an initial tank pressure of approximately 1800 psig would yield the desired final wing (and tank) pressure of approximately 180 psig. Mass flow rate, and thus wing inflation rate, was strongly dependent on the regulator set point, and therefore wing inflation rate was controllable by means of the regulator pressure set point.

Laboratory testing was used to find the regulator set point corresponding to the desired wing inflation rate. In order to limit the number of inflation cycles conducted with the actual wings, a rigid pressure vessel with volume equivalent to the inflatable wings was used as a wing simulator. Figure 8 shows the pressure time history within this wing simulator as a function of the regulator pressure set point. The maximum allowable inflation rate was specified by the wing manufacturer. The desired inflation rate was determined from simulation, indicating the required load factor as a function of time for a pullout from a ballistic trajectory. Based on these test results, a regulator set point of 500 psig was selected for the in-flight inflation operations.

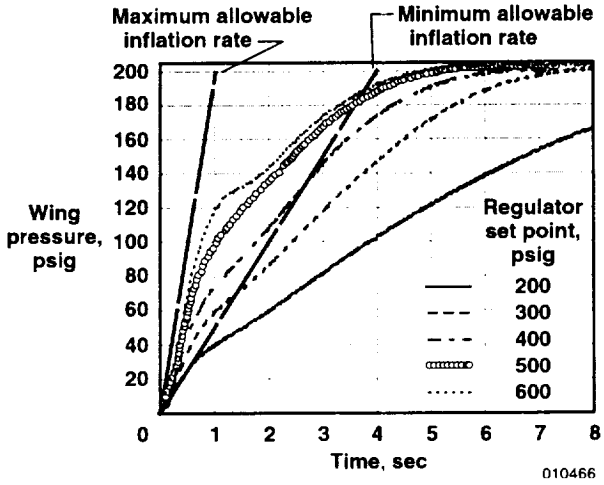

Figure 8. Wing inflation pressure time history as a function of regulator set point.

Wing Stowage and Retention Subsystem Design

For in-flight inflation operations, the I-2000 research vehicle with its wings deflated and stowed was carried to its release altitude mated with the air-launch carrier aircraft (fig 9). A system was required for stowing and retaining the deflated wings while the research vehicle was mated with the air-launch carrier aircraft and while the research vehicle was in ballistic flight prior to wing inflation. For the I-2000, there was no requirement for the deflated wings to be stowed within the body of the vehicle. Figure 10 shows the I-2000 vehicle with the

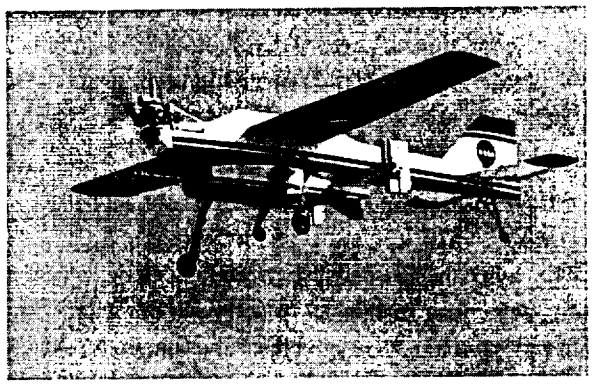

Figure 9. I-2000 research vehicle mated with air-launch carrier aircraft.

wings in both stowed and inflated configurations. Each wing panel was z-folded from the wingtip and the stowed structure was retained along the side of the fuselage with a horizontal fabric strap. Each fabric strap

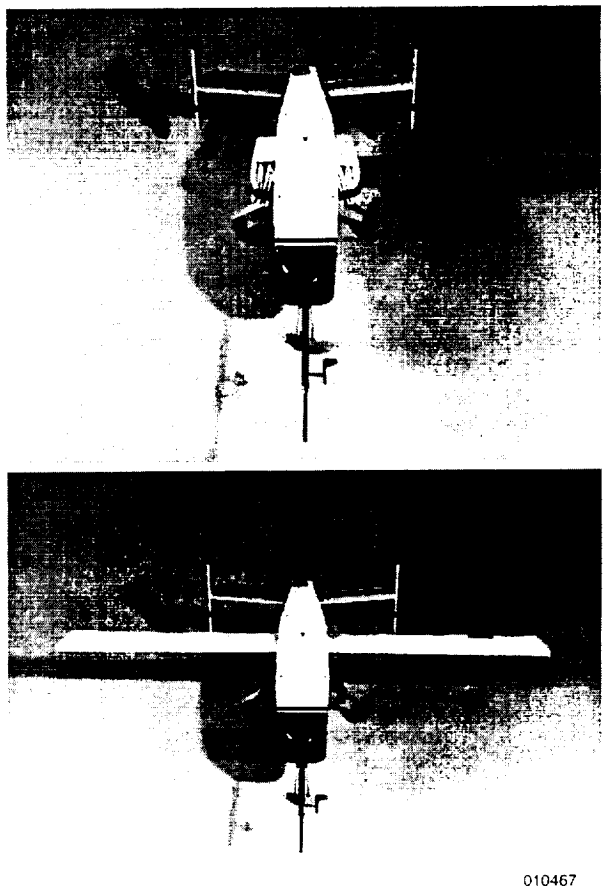

Figure 10. Photo comparison of I-2000 with wings stowed (top) and inflated (bottom).

was fixed to the fuselage at its front and was terminated with a loop at the aft end. Each loop end was retained by a pin driven by a small pneumatic actuator mounted on the fuselage just aft of the stowed wing assembly.

Inflation System Integration and Testing

The inflation gas subsystem and the wing stowage subsystem were integrated to form the complete wing inflation system. A schematic of the integrated system is shown in figure 11. The primary objective of the wing inflation system integration was to reliably control the relative timing of the wing-retention pin release and the wing inflation valve opening. The timing objective was for pin release to occur 100 msec (±50 msec) prior to valve opening. Two small pneumatic cylinders actuated the wing retention pins and one larger pneumatic cylinder actuated the wing inflation valve. Two small mechanically driven spool valves controlled the flow of low-pressure (120 psig) actuation gas to the pneumatic cylinders. Two small servoactuators drove the spool valves. Relative timing of wing-retention pin release and wing inflation valve opening was controlled by modifying the relative timing of the command signal to the separate servoactuators.

Extensive ground testing was used to adjust the relative timing, using the wing simulator to replace the actual wing test article. Finally, a single ground test of the integrated in-flight inflation system was done for flight qualification.

Airborne Systems and Instrumentation

The research vehicle was equipped with a COTS command-uplink radio control (R/C) system. The ground research pilot kept the research vehicle in direct sight throughout each flight operation, and controlled all aspects of the research mission with a COTS uplink control computer-transmitter. Control surface gains, throws, and interconnects, as well as stick shaping and trim capability were available to the research pilot through the computer-transmitter. Onboard systems included a receiver-computer, conventional R/C servoactuators, and redundant battery power systems. No additional stability augmentation or rate damping was implemented onboard the research vehicle.

The vehicle was instrumented for flight dynamics, performance, and subsystem health measurements. The core of the instrumentation system was a small COTS single-board microcontroller-based data-logging engine. This system was supplemented with power

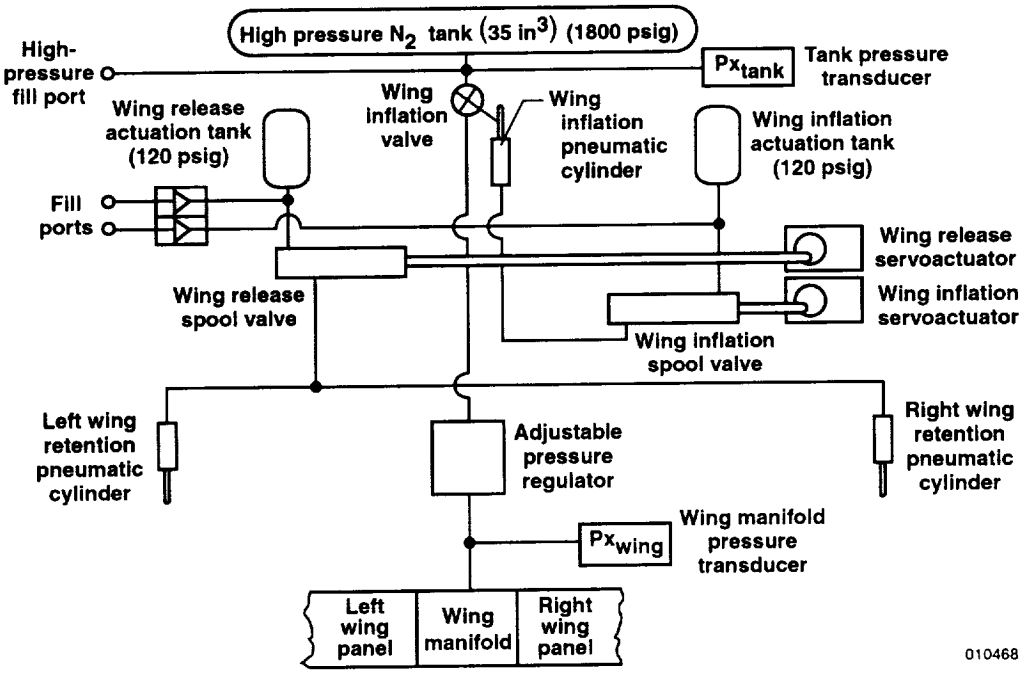

Figure 11. Schematic of the integrated in-flight-inflation system.

conditioning and signal conditioning circuit boards appropriate for the analog transducers used. During each flight operation, research data were logged to onboard system memory, and the data were downloaded to a laptop computer at the end of each flight for further processing and analysis. There was no downlink system for the flight data.

Instrumentation selection was driven by availability and the desire to minimize weight, power required, and cost. All instrumentation components were COTS units. Each control surface position was instrumented with a control-position transducer. All airdata measurements were made with a small airdata probe. On the probe, angle of attack (α) and angle of sideslip (β) were instrumented with vane-driven potentiometers. Pitot and static ports on the probe were plumbed with tubing to absolute (static) and differential (pitot minus static) piezoresistive pressure transducers mounted in the vehicle body. Body-axis angular rates were measured with ceramic Coriolis-effect rate transducers, and body-axis acceleration measurements were made with a triaxial piezoresistive accelerometer package. Vehicle attitude was not directly measured; postflight trajectory reconstruction was used to synthesize vehicle pitch attitude during wings-level flight by using measured altitude rate and α. High-pressure tank and wing inflation pressure measurements were made with piezoresistive gage pressure transducers fabricated in stainless steel enclosures.

Prior to the initiation of flight operations, the electromagnetic interference (EMI) susceptibility of the uplink-command system to the additional onboard systems was measured through a standard range-test procedure. Initial range testing identified the need for an EMI-shielded enclosure on the instrumentation system, which was then implemented.

Vehicle Inertia Swings

Analysis of flight data and development of a simulation required accurate measurement of the vehicle inertial properties. A bifilar pendulum suspension technique[15] was used to experimentally measure the vehicle moments of inertia and the cross products of inertia. The bifilar suspension approach (fig 12) allows four degrees of freedom and allows simultaneous identification of multiple moments of inertia and cross products of inertia with a single suspension geometry. Three separate orthogonal suspension orientations were used to identify the important components of the inertia tensor. The different suspension orientations allowed comparison of the measured inertia tensor components from different experiments, improving confidence in the results.

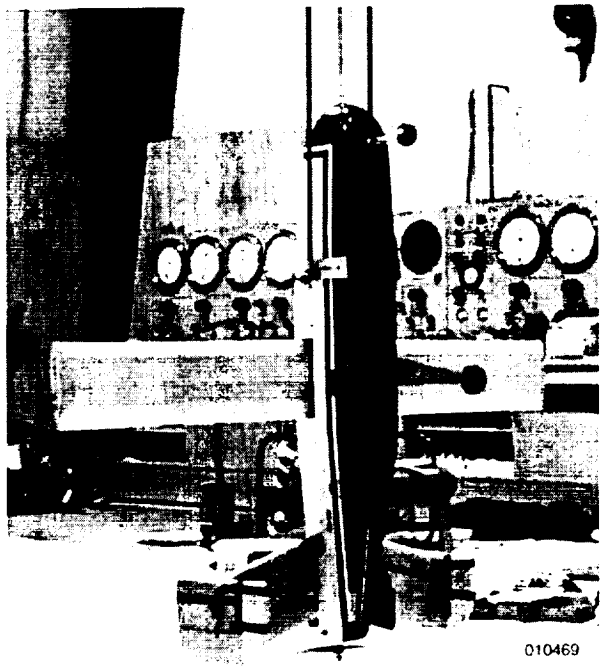

Figure 12. Test configuration for inertia swing on I-2000 (suspension lines exaggerated for clarity).

The onboard data system was used to record body-axis rates during the suspension experiments, and parameter estimation techniques were used to estimate the inertia components. All inertia components were corrected for the mass of the suspension hardware used. Table 1 presents the inertia swing results for two of the flight configurations.

Table 1. Measured research vehicle inertias.

Inertia Component	Rigid Wing Configuration	
	Average, slug-ft^2	Standard Deviation, slug-ft^2
Ix	0.1701	0.0112
Iy	0.7647	0.0046
Iz	0.8776	0.0018
Ixy	-0.0009	0.0038
Ixz	0.0515	0.0086

Table 1. continued.

Inertia Component	Preinflated Wing Configuration	
	Average, slug-ft^2	Standard Deviation, slug-ft^2
Ix	0.2290	0.0101
Iy	0.7186	0.0010
Iz	0.8970	0.0045
Ixy	0.0045	0.0062
Ixz	0.0378	0.0106

Flight Test Approach

All flight piloting was performed by an expert-class ground-based pilot using line-of-sight visual cues only. Ground and flight operations involving pressurized systems were briefed beforehand, and safety zones around the aircraft were restricted to essential personnel.

The flight test approach of the I-2000 followed a conservative build-up approach commonly used in developmental flight testing. The objectives of the initial flights were to develop the operational procedures, to wring out the airframe (adjust control system gains and control surface throws, optimize engine performance, adjust gear geometry), and to check out the instrumentation system. The initial flights were made in the powered configuration and at minimum weight in order to minimize flight loads and to minimize takeoff and landing speeds. Furthermore, for the initial flights the vehicle was configured with the rigid wing in order to eliminate risk to the unique inflatable flight-test article.

Following the initial checkout flights, several research flights were flown in the rigid-wing configuration. The objective of these flights was to document the trim, performance, and stability and control characteristics of the I-2000 vehicle in its baseline rigid-wing configuration. These research flights were also used to develop and practice some of the flight-test maneuvers planned for flight with the inflatable wing. During these research flights, the instrumentation system collected data for postflight analysis. The research maneuvers executed included doublets for stability and control derivative estimation, and pushover-pullup (POPU) maneuvers for trim and performance measurement. During this first flight series, the vehicle weight was also increased in one-pound increments until the maximum expected flight weight was reached. Finally, the powered, rigid-wing configuration was used to simulate and practice the maneuver sequence planned for the air-launched, unpowered, in-flight-inflated configuration flights.

Following the initial series of research flights in the powered, rigid-wing configuration, the vehicle was modified and flown in the powered, preinflated-wing configuration. For these research flights, the inflatable wing was inflated on the ground several minutes prior to takeoff, and the onboard pressure systems were used to maintain wing pressure at approximately 180 psig. During this preinflated flight series, research maneuvers included longitudinal doublets for stability and control derivative estimation, and POPUs for trim and performance measurement.

After all research objectives were met with the I-2000 in the powered, preinflated-wing configuration, the vehicle was prepared for unpowered air-launched flights with in-flight inflation of the wing. The engine and all associated hardware were removed from the vehicle and the in-flight inflation system hardware was installed. A hook was installed in the top of the wing-deck assembly for mating to the belly of the air-launch carrier aircraft. One captive-carry flight was conducted in the mated configuration to practice air-launch operational procedures and to confirm the release-point flight conditions. Following the captive-carry flight, three flights were made with air launch and in-flight inflation of the wing. Because the duration of these unpowered flights was short, no intentional research maneuvers were performed.

Flight Data Results

Rigid Wing Compared to Inflatable Wing

The available flight data allowed comparison of the lift-generating capability and the trim curve of the aircraft in three different configurations: the rigid wing, the preinflated wing, and the in-flight inflated wing. The first two configurations were powered while the last was unpowered. To minimize the effect of unknown (i.e. unmeasured) engine thrust, normal force coefficient was used for the comparison rather than lift coefficient because the thrust axis was perpendicular to the vehicle normal axis.

To make the comparison of the different configurations most meaningful, only selected subsets of the flight data were used. There were three criteria for selecting the flight data for this comparison: power setting, symmetric elevon rate, and roll rate. For the powered configurations, only flight data with idle-power throttle settings were used; for the unpowered configuration, all data were available. For flights with POPU maneuvers flown, that portion of each POPU with a smooth and slow (target of 1 deg/sec) symmetric elevon rate during the pullup portion were used. Similar criteria were used to screen flights that did not contain intentional POPU maneuvers. Finally, only flight data with small roll rates were used. Given these selection criteria, portions of four flight data sets were available for comparison.

Normal force coefficient was calculated from the flight-measured normal accelerometer and dynamic pressure measurements, and the configuration-specific vehicle weight:

$$C_N = a_n * mg / (\bar{q} * S_{ref}) \qquad (1)$$

Figure 13 shows a comparison of the vehicle normal-force coefficient as a function of α for the three configurations. For the α range spanned in the analysis,

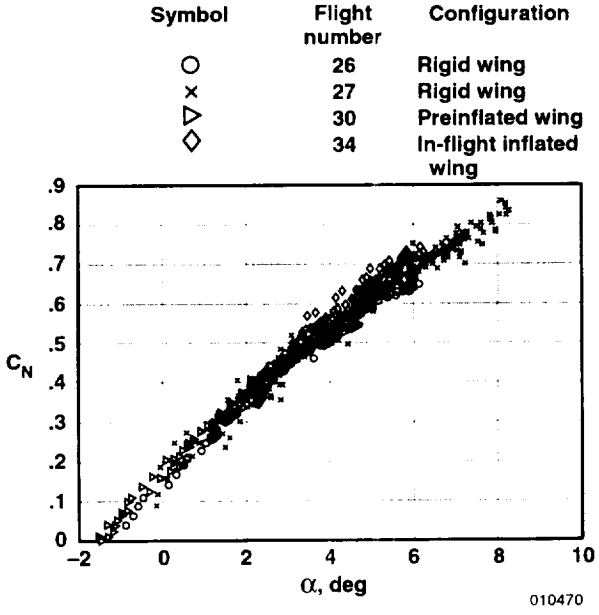

Figure 13. Normal force coefficient as a function of α for three configurations.

the flight data show that the lift-generating capability of the vehicle is repeatable across the three configurations. These data also demonstrate that the rigid-wing configuration can be an effective simulator of the inflated configurations.

Figure 14 shows a comparison of the vehicle trim curve (α as a function of symmetric elevon) for the same flight data subsets shown in figure 13. For the

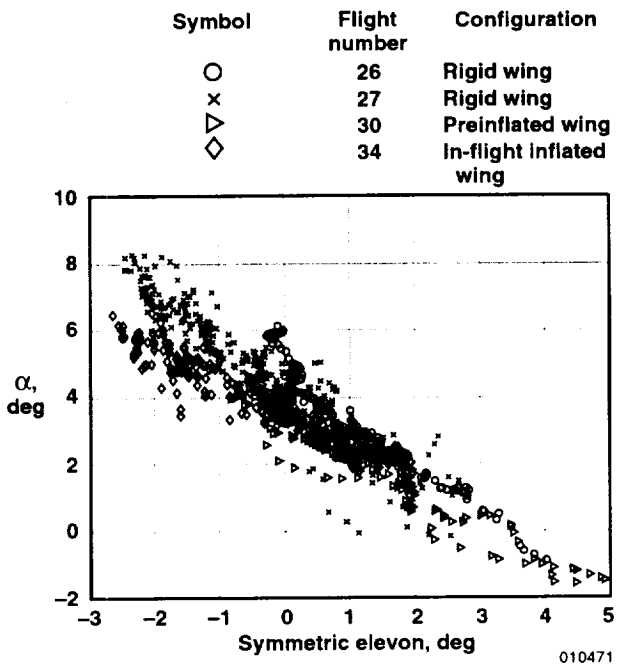

Figure 14. Trim curve for three configurations.

trim range spanned in the analysis, the rigid-wing and preinflated-wing configurations show steeper (larger negative slope) trim curves than the in-flight-inflated configuration. The steeper trim curves are consistent with larger symmetric elevon effectiveness. Given that figure 13 showed no significant difference in the lift-generating capability of the three configurations, the source of the trim curve difference is more likely attributed to the removal of the engine rather than a difference in the aerodynamics of the in-flight inflated wing. By removing the engine for the in-flight-inflated configurations, the entrained flow over the control surfaces was reduced, thereby reducing their effectiveness.

Roll trim of the rigid-wing and preinflated-wing configurations was measurably different. With respect to the rigid-wing configuration, the initial flight with the

preinflated wing required approximately an additional 10 degrees of differential elevon to trim. Postflight measurements of the wing revealed that when inflated, the wing had a small amount of twist unintentionally built into each wing panel. For all subsequent flight activity, a small trim tab was affixed to the left wing panel to correct the roll trim.

Parameter Estimation Results for Simulation Development

The initial aerodynamic model used for simulation was developed analytically using a vortex-lattice panel code[16]. An update of this initial aerodynamic model with flight-derived results was desirable in order to improve the fidelity of the simulation for flight-planning purposes. Specialized flight-test maneuvers (i.e. doublets and POPUs) were flown to support this objective. Analysis of both the short-period (i.e. longitudinal doublet) maneuvers and the larger-scale (i. e. POPU) maneuvers allowed updating the important parameters of the aerodynamic model. Longitudinal stability and control parameters were extracted from both the longitudinal doublet and the POPU maneuvers using a standard time-domain output-error parameter estimation code.[17]

Figure 15 compares the flight-measured and computed time history for one longitudinal doublet maneuver analyzed for the rigid-wing configuration. Owing to the large horizontal tail and the low flight speed, the short-period mode is heavily damped -- no free oscillation is apparent after the pilot control motion (symmetric elevon) is stopped. This maneuver, performed in level flight with significant engine thrust maintaining speed and altitude, provided good estimates of the primary stability and control parameters--normal-force curve slope parameter (C_{N_α}), longitudinal stability parameter (C_{m_α}), and symmetric elevon control effectiveness parameter ($C_{m_{\delta e}}$). However, because engine thrust was not measured, it was not possible to identify the important axial force parameters.

Analysis of the POPU maneuvers, which span a larger range of the flight envelope (airspeed, α, lift coefficient, etc.) allows extraction from flight data of some of the remaining axial force parameters. The POPU maneuvers were flown with the engine at an idle-thrust setting to minimize unknown thrust contributions. Hence, the axial-force parameter estimates extracted

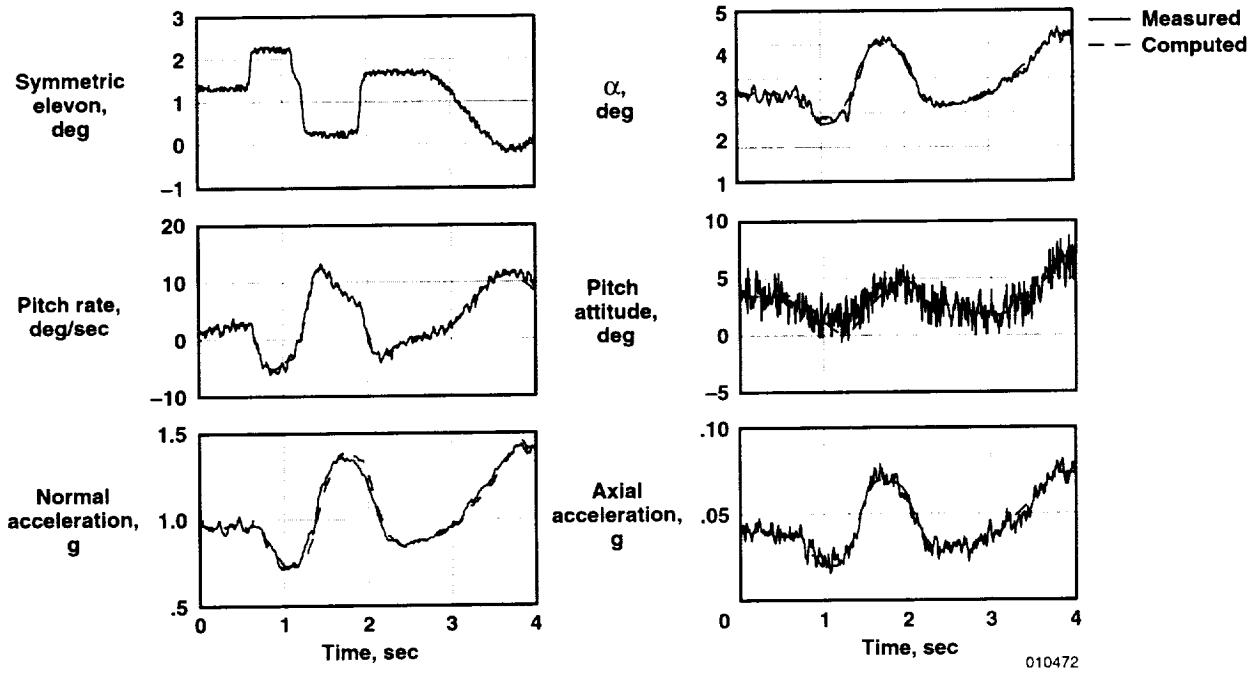

Figure 15. Comparison of flight-measured and computed time history results for a longitudinal doublet in rigid-wing configuration.

from the POPU maneuvers are more reliable than those from analysis of the longitudinal doublet maneuvers.

Figure 16 compares the flight-measured and computed time histories for one POPU maneuver analyzed for the preinflated configuration. The large excursions in airspeed, α, normal acceleration, and pitch attitude were expected to be representative of those observed in the first in-flight inflation of the I-2000.

Analysis of several longitudinal doublet and POPU maneuvers yielded an updated set of longitudinal stability and control parameters for use in the flight planning simulation. Table 2 compares the preflight (analytically-derived) and flight-estimated values of the primary stability and control parameters--C_{N_α}, C_{m_α}, $C_{m_{\delta e}}$. The flight-determined estimate of normal-force curve slope, C_{N_α}, was nearly identical to the preflight prediction. However, the flight-determined estimate of the longitudinal stability parameter, C_{m_α}, showed lower stability than the preflight prediction, and the flight-determined estimate of the symmetric elevon control effectiveness parameter, $C_{m_{\delta e}}$, showed slightly higher effectiveness than the preflight estimate.

Table 2. Comparison of analytical and flight-estimated aerodynamic model parameters.

Parameter	Preflight Prediction	Flight Estimate
	(deg^{-1})	(deg^{-1})
C_{N_α}	0.110	0.105
C_{m_α}	-0.044	-0.025
$C_{m_{\delta e}}$	-0.034	-0.040

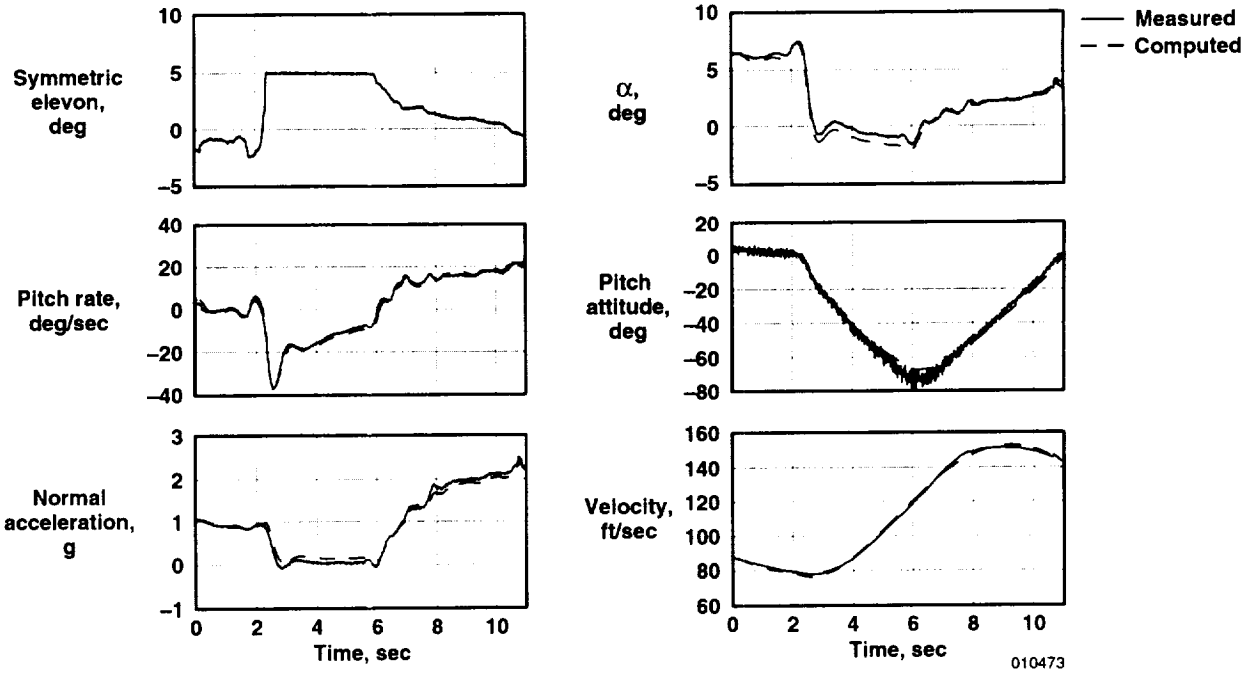

Figure 16. Comparison of flight-measured and computed time history results for a POPU maneuver in the preinflated-wing configuration.

In-flight Inflation

Three flight operations were conducted to demonstrate the in-flight inflation capability of the I-2000 and to document the wing and vehicle dynamic response during inflation and transition to lifting flight. Figure 17 shows a sequence of six photographic images documenting the air launch of the I-2000 from the carrier aircraft and the subsequent wing inflation. The time listed below each image is only the approximate value, estimated by correlating photographic, video, and onboard measurements, and using a common time scale for all data sources. Figure 18 shows a time history of some of the pertinent onboard measurements.

Release from the carrier aircraft occurred at 26.9 sec (fig. 18, normal acceleration) at a dynamic pressure of approximately 11 lb/ft^2 (fig 18, dynamic pressure), and the I-2000 was in ballistic flight for about 1 sec (fig 17, photos 1 and 2). During ballistic flight the research pilot made no control input to the I-2000 beyond the command to initiate the wing inflation sequence. During this time, the dynamic response is primarily a roll to the right (fig 18, roll rate). The low roll inertia of the I-2000 (with the wings stowed) coupled with propeller swirl from the carrier aircraft, impart the roll rate. Some pitching motion is also apparent in the data.

Shortly before 27.9 sec, the research pilot commanded wing inflation, and at 27.9 sec, the wing-retention straps were released. In figure 17, photo 3 shows the wing retention straps just after release, retracting forward. At 28.05 sec the pressure began to rise in the wing (fig 18, wing pressure) as it inflated (fig 17, photo 4). As the wing unfolded and inflated, the inertial and aerodynamic effects of the wings generated significant and dynamic rolling moments and heaving forces, as shown by the roll rate and normal acceleration measurements. Although the photos indicate a symmetric wing deployment (fig 17, photos 4 and 5), roll rate peaked at –250 deg/sec and normal acceleration peaked at 2*g*. Moments and forces in the remaining axes were relatively small. The angles of attack and of sideslip induced during the unfolding and inflation were small and well-damped; no indications of divergence or instability were evident.

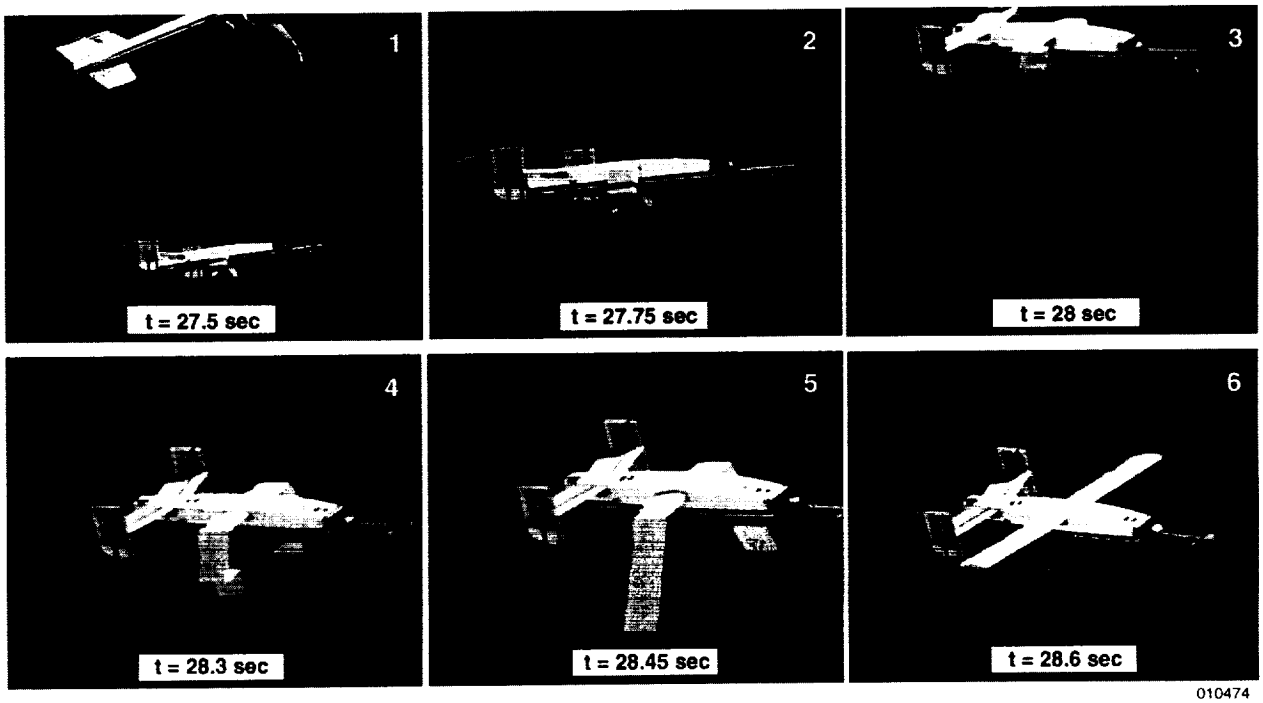

Figure 17. Photo sequence of air launch and wing inflation.

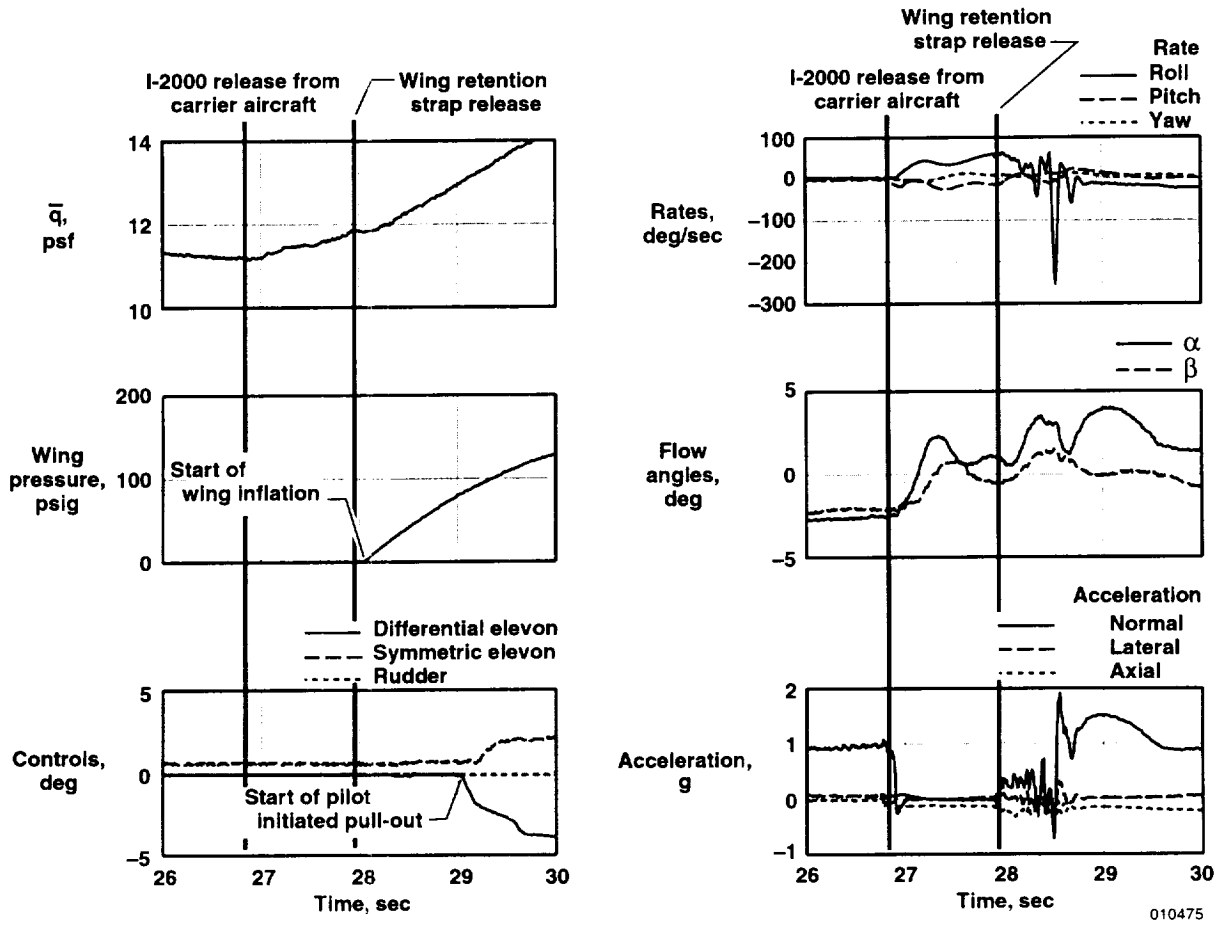

Figure 18. Time history of air launch and wing inflation.

At approximately 28.6 sec the wing reached its final inflated shape (fig 17, photo 6) at a wing pressure of approximately 55 psig. The aerodynamic roll damping of the winged aircraft was now sufficient to damp out all high-frequency dynamic motions. From 28.65 sec forward, the α and normal acceleration time histories show significantly stronger correlation than that during the inflation process. This is strong evidence that the wing is fully inflated and capable of generating significant aerodynamic lift force. As the wing pressure continued to rise toward the final value of 180 psig, the research pilot assumed control of the aircraft, and flew the vehicle to an unpowered landing.

Conclusions

Ground and flight test techniques traditionally applied to large-scale research aircraft were successfully applied to a small-scale research aircraft configured with an inflatable wing at the NASA Dryden Flight Research Center (Edwards, California). The aircraft was flown in a powered configuration with a rigid wing and then with an inflatable wing. It was also air-launched in an unpowered configuration in which the wing was inflated in flight. Based on the research results to date, the following conclusions have been drawn:

1. Recent advances in miniaturized instrumentation technology have made it possible to obtain quantitative flight research results from aircraft at small scale. Research data quality was sufficient to allow application of parameter estimation flight test techniques.

2. Mechanics of materials analytical methods were effective in modeling the multiple-spar wing configuration for a range of inflation pressures.

3. Integration of the inflatable wing test article into a research aircraft configuration is possible at small scale.

Powered flight, using only the control surfaces on the tail of the aircraft, was demonstrated.

4. For the angle-of-attack range spanned in the flight program, the flight data demonstrated the rigid-wing configuration to be an effective simulator of the inflatable-wing configurations.

5. The asymmetric twist distribution of the inflatable wing required significant differential elevon deflection to achieve trimmed flight. A small trim tab on one wing was sufficient to achieve trimmed flight.

6. The feasibility of ballistic airdrop and inflight inflation of the wing, with transition to controlled lifting flight, was demonstrated in three flight operations. Wing inflation and transition to lifting flight was rapid; vehicle dynamic response was benign and limited primarily to roll and heave motions. No indications of instability or divergence were evident.

Acknowledgment

The authors would like to thank Mr. John Fraysse of the U.S. Navy for making the inflatable wings available to NASA-Dryden. Without the inflatable wing test articles, this research would not have been possible.

References

[1]U.S. Department of Commerce, Patent and Trademark Office, Arlington, Virginia, U.S. Patent, 1,905,298, Taylor McDaniel, *Flying Machine*, April 25, 1933.

[2]Stadvec, Ernest, *The Inflatoplane*, published by Essco, Akron, Ohio, February, 1980.

[3]Cocke, Bennie W., Jr., *Wind-Tunnel Investigation of the Aerodynamic and Structural Deflection Characteristics of the Goodyear Inflatoplane*, NACA-RM-L58E09, September 10, 1958.

[4]Whitney, Richard V., "Goodyear's Inflatoplane and Project Wagmight," *Journal, American Aviation Historical Society*, Summer 2000, pp. 104-110.

[5]*Jane's All the World's Aircraft, 1955-1956*, compiled and edited by Leonard Bridgman, McGraw-Hill, 1956, p. 90.

[6]Wade, Mark, "FIRST Re-Entry Glider," *Encyclopedia of Aeronautics*, on the Web at http://www.friends-partners.org/mwade/craft/firlide.htm 7/2/01.

[7]U.S. Department of Commerce, Patent and Trademark Office, Arlington, Virginia, U.S. Patent 3,944,169, James R. Bede, *Hang Glider*, March 16, 1976.

[8]U.S. Department of Commerce, Patent and Trademark Office, Arlington, Virginia, U.S. Patent 3,957,232, Wayne A. Sebrell, *Inflatable Wing*, May 16, 1976.

[9]U.S. Department of Commerce, Patent and Trademark Office, Arlington, Virginia, U.S. Patent 6,082,667, Roy Haggard, *Inflated Wings*, July 4, 2000.

[10]Crimi, Peter, "Divergence of an Inflated Wing," *Journal of Aircraft*, vol. 37, no. 1, January-February 2000, pp. 184-186.

[11]Brown, Glen, Roy Haggard, and Brook Norton, "Inflatable Structures for Deployable Wings," AIAA-2001-2068, *A Collection of the 16th AIAA Aerodynamic Decelerator Systems Technology Conference and Seminar*, Boston, Massachusetts, 21-24 May 2001, pp. 19-26.

[12]Leonard, Robert W., George W. Brooks and Harvey G. McComb, Jr., *Structural Considerations of Inflatable Reentry Vehicles*, NASA TN D-457, September 1960.

[13]Comer, R.L. and Samuel Levy, "Deflections of an Inflated Circular Cylinder Cantilever Beam." *AIAA Journal*, vol. 1, no. 7, July 1963, pp. 1652-1655.

[14]Webber, J.P.H., "Deflections of inflated cylindrical cantilever beams subjected to bending and torsion," *The Aeronautical Journal*, vol. 86, no. 858, October 1982, Paper 1020, pp. 306-312.

[15]de Jong, R. C., and J. A. Mulder, "Accurate Estimation of Aircraft Inertia Characteristics from a Single Suspension Experiment," *Journal of Aircraft*, vol. 24, no. 6, June 1987, pp. 362-370.

[16]Margason, Richard J., and John E. Lamar, *Vortex-Lattice FORTRAN Program for Estimating Subsonic Aerodynamic Characteristics of Complex Planforms*, NASA TN D-6142, February 1971.

[17]Murray, James E., and Richard E. Maine, *pEst Version 2.1 User's Manual*, NASA TM 88280, September 1987.

REPORT DOCUMENTATION PAGE

Form Approved
OMB No. 0704-0188

1. AGENCY USE ONLY (Leave blank)	2. REPORT DATE	3. REPORT TYPE AND DATES COVERED
	January 2002	Technical Memorandum

4. TITLE AND SUBTITLE

Ground and Flight Evaluation of a Small-Scale Inflatable-Winged Aircraft

5. FUNDING NUMBERS

274-00-00E8-RR-00-DDF

6. AUTHOR(S)

James E. Murray, Joseph W. Pahle, Stephen V. Thornton, Shannon Vogus, Tony Frackowiak, Joe Mello, Brook Norton

7. PERFORMING ORGANIZATION NAME(S) AND ADDRESS(ES)

NASA Dryden Flight Research Center
P.O. Box 273
Edwards, California 93523-0273

8. PERFORMING ORGANIZATION REPORT NUMBER

H-2471

9. SPONSORING/MONITORING AGENCY NAME(S) AND ADDRESS(ES)

National Aeronautics and Space Administration
Washington, DC 20546-0001

10. SPONSORING/MONITORING AGENCY REPORT NUMBER

NASA/TM-2002-210721

11. SUPPLEMENTARY NOTES

Presented at the 40th AIAA Aerospace Sciences Meeting & Exhibit, 14-17 January 2002, Reno, Nevada.

12a. DISTRIBUTION/AVAILABILITY STATEMENT

Unclassified—Unlimited
Subject Category 05

12b. DISTRIBUTION CODE

13. ABSTRACT (Maximum 200 words)

A small-scale, instrumented research aircraft was flown to investigate the flight characteristics of inflatable wings. Ground tests measured the static structural characteristics of the wing at different inflation pressures, and these results compared favorably with analytical predictions. A research-quality instrumentation system was assembled, largely from commercial off-the-shelf components, and installed in the aircraft. Initial flight operations were conducted with a conventional rigid wing having the same dimensions as the inflatable wing. Subsequent flights were conducted with the inflatable wing. Research maneuvers were executed to identify the trim, aerodynamic performance, and longitudinal stability and control characteristics of the vehicle in its different wing configurations. For the angle-of-attack range spanned in this flight program, measured flight data demonstrated that the rigid wing was an effective simulator of the lift-generating capability of the inflatable wing. In-flight inflation of the wing was demonstrated in three flight operations, and measured flight data illustrated the dynamic characteristics during wing inflation and transition to controlled lifting flight. Wing inflation was rapid and the vehicle dynamics during inflation and transition were benign. The resulting angles of attack and of sideslip were small, and the dynamic response was limited to roll and heave motions.

14. SUBJECT TERMS

Research aircraft, Inflatable gliders, Aircraft performance, Inflatable structures, Structural analysis

15. NUMBER OF PAGES

24

16. PRICE CODE

17. SECURITY CLASSIFICATION OF REPORT	18. SECURITY CLASSIFICATION OF THIS PAGE	19. SECURITY CLASSIFICATION OF ABSTRACT	20. LIMITATION OF ABSTRACT
Unclassified	Unclassified	Unclassified	Unlimited